Dielectrophoretic Trapping in Paper: Paper-based Electric Field Gradients for High-Throughput Particle Trapping

Md. Nazibul Islam, Zachary R. Gagnon*
Artie McFerrin Department of Chemical Engineering, Texas A&M University, USA. E-mail: zgagnon@tamu.edu

Abstract

Dielectrophoresis (DEP) is a phenomenon which utilizes a spatially varying electrical field to induce forces on suspended polarizable matter, including particles and cells. Such field non-uniformities are conventionally created using a wide variety of conductive electrode arrays. Alternatively, insulator based dielectrophoresis (iDEP) uses small micron-scale insulating structures to generate high electric field gradient that can used to selectively trap, isolate and concentrate biomolecules such as bacteria, virus, red blood cells, cancer cells etc. Despite significant advances in microfabrication technology, the commercial adoption of iDEP based devices remains elusive. One reason for such low market penetration is a lack of low-cost and scalable fabrication methods to quickly micro-fabricate these insulating structures required for iDEP. We propose here that paper-based devices can offer a low-cost, easy to use alternative to traditional iDEP devices. In this article, we demonstrate for the first time the ability to perform iDEP particle trapping using the naturally occurring insulating porous structures of paper. In particular, we use polymeric laminated nonwoven fiberglass paper channels as a source of insulating structures for iDEP. We apply a flow of polarizable microparticles directly within the nonwoven channel and simultaneously drop a pulsed DC electric field perpendicular to the flow direction. We show the ability to trap particles by DEP using an applied voltage as low as 2V using two different flow mechanisms: constant fluid flow rate using an external pump and passive fluid flow by capillary wicking. Using a combination of micro computed tomography and finite element analysis, we then present a computational model in order to probe the micro-scale DEP force formation dynamics within nonwoven structure. This new iDEP platform enables the development of robust, low-cost, and portable next generation iDEP systems for a wide variety of sample purification and liquid handling applications.

1. Introduction

Insulator-based dielectrophoresis (iDEP) has emerged as an electrokinetic tool for high-throughput, selective manipulation of biomolecules for robust and portable micro total analysis systems (μTAS, or lab-on-a-chip). The iDEP method itself utilizes an organized array of insulating structures in order to induce local curvature in the electric field lines which pass across these objects. Such curvature induces a local electric field gradient and a subsequent dielectrophoretic force. These forces can then be used to trap suspending particles, cells and biomolecules in the surrounding flow field. The first report on iDEP-based manipulation of biomolecules was published in 1989, where Masuda et al. used a set of insulating pillar structures to dielectrophoretically trap two cell species and subsequently apply a pulsed voltage to initiate cellular fusion [1]. The next significant breakthrough was in 2000 when Cummings and Singh reported a novel microdevice that contained a set of equally spaced insulating posts etched in a glass microchannel. This

device was used to demonstrate for the first time, distinct regimes of streaming DEP and trapping DEP which was achieved by controlling the ratio between linear electro-osmotic and dielectrophoretic forces using an externally applied DC electric field [2]. In 2002, Chia-Fu Chou et al. coined the term “electrodeless dielectrophoresis” where the authors demonstrated DEP trapping of single and double stranded DNA using insulating constrictions and by applying an AC electric field [3]. The insulating structures allowed DEP trapping at a lower frequency that could not be achieved using metal electrodes due to electrolysis on electrode surface [3]. Since then, several groups have contributed into the development of iDEP technology and demonstrated its utility across a wide range of sample processing applications. The Lapizco-Encinas group, for example, has studied the effects of suspending media conductivity and pH and electrode geometry on particle trapping using equally spaced insulating posts [4,5]. The same group has also reported iDEP based biomolecule concentration and separation using bacterial and yest cells [6]. Recently, the Lapizco-Encinas group has reported an iDEP-cascading device that integrate a prescreening stage with an analysis stage to remove large cellular debris before concentrating and purifying a biomolecule [7]. The Minerick research group has reported a DC-iDEP device that uses a rectangular insulating obstacle embedded in a microchannel to investigate the DEP response of human blood types [8]. Further structural innovations arose from the Davalos group where they developed several contactless electrode-based iDEP devices where the electrodes themselves are separated from the microchannel containing the insulating pillar arrays by a thin PDMS membrane and employed these devices to demonstrate biomedical applications such as, isolation of live and dead cells, screening of ovarian cancer cells and isolation of prostate tumor initiating cells [9–12]. Other research groups have experimented with varying the shape and geometry of the insulating structures themselves. The Hayes research group has developed iDEP devices based on “saw-tooth” geometric gradients which use microchannel walls with pointed triangular teeth-linke patterns as the insulating field curvature-inducing structures [13]. These saw-tooth devices have been used to demonstrate selective manipulation of bacterial species, concentration of viruses, trapping of Aβ amyloid fibrils and separation of human blood cells and biomarkers [14–17]. In addition, the Ros group has utilized streaming DEP, where free-flowing particles and biomolecules are concentrated spatially as the flow continuously across insulating structures. Streaming DEP has been successfully used to develop size dependent, high throughput devices for continuous separation of protein nanocrystals and DNA molecules [18–20].

While iDEP offers the potentially for low-cost rapid sample processing across a wide range of samples and applications, major disadvantage of these traditional microfluidic iDEP devices is that the high electric field gradient required for DEP trapping is generated by insulating microstructures that are typically created in a microfabrication cleanroom. Georg R. Pesch and co-researchers worked to overcome this disadvantage by designing iDEP devices using naturally porous materials [21–23]. These novel iDEP devices use the insulating microstructures that exist within macroscopic porous materials in order to generate the same regions of high electric field gradients that are conventionally produced with microfabricated pillar arrays. Such a method has been used to as a high throughput iDEP filtration system to separate polystyrene (PS) particles and biomolecules (*S. cerevisiae*, yeast) at a flowrate that is several orders of magnitude higher than most

microfluidic iDEP devices [21–23]. Despite these significant academic advances, commercial adoption of iDEP-based devices remains low. One reason for such limited adoption is a lack of low-cost manufacturing methods capable of scalable production of these fluidic chips with small micron-scale insulating pillars. While techniques such as injection molding are capable of scalable production, they often require a six-figure upfront capital investment for both the development and the production phases of commercialization. Such high commercialization costs can constraint and severely limit the academic translation, and widespread consumer adoption of iDEP-based technology. Therefore, a low-cost and scalable iDEP device manufacturing method will have significant impact in democratizing innovation in this research area.

Over the past decade, paper-based microfluidics has received significant interest for use in ultra-low-cost diagnostics [24]. Conventionally powered passively by liquid wicking, paper-based devices have been extensively developed for lateral flow assays and colorimetric detection devices [25–27]. In addition, several groups have integrated electrokinetics based applications such as electrophoresis and isotachophoresis on paper [28–31]. The Chakraborty research group has demonstrated several applications using paper and pencil based electrokinetic microdevices and in 2019 they reported particle manipulation on paper using conventional electrode-driven DEP using a pair of pencil-based electrodes [28,32,33]. In this device, an electric field was applied across a small paper gap using a pair of pencil-drawn electrodes in order to dielectrophoretically maneuver PS particles on a cellulose filter paper [33]. The particles were observed to move from zones of high electric field to low electric field as were defined by the electrodes themselves. In addition, *E. coli* was concentrated near the positive electrode using negative DEP to demonstrate viability of the device for biological applications [33].

In this work, we report a novel insulator based dielectrophoretic technique that uses paper fibers themselves as the insulating structures for iDEP. We used a synthetic fiber paper, typically described as a “nonwoven” which is comprised of fiberglass fibers. The material itself, Craneglas® 230 is fabricated using electrical grade glass fibers that act as electrical insulators [34,35]. We used our recently published low-cost pressurized flow mechanism called microfluidic pressure in paper (µPiP) to fabricate paper fluidic devices and experimentally demonstrate iDEP particle trapping in craneglas paper pores. First, we use a CO_2 laser to rapidly cut fluidic channels from a sheet of crane glass paper. We then confine these paper channels with a pair of adhesive copper tape electrodes between two thin and flexible laminating PDMS membranes. Using a combination of corona plasma treatment and a benchtop thermal press, we confine and irreversibly seal these channels within the membranes. We then use syringe pump to flow fluorescently labeled PS particle solution through paper. We apply a pulsed DC electric field across paper channel perpendicular to the flow direction and the insulating paper fibers are observed to serve as sources of high electric field gradient, which we call “trapping zones”, that are observed to locally trap particles by iDEP. We also utilize micro-CT scan images of the craneglas paper channel to digitize this material geometry for use with a finite element (FE) model of the electric field distribution to computationally study the formation of localized trapping zones within the paper. We use fluorescent microscopy to measure particle trapping within the paper channels and compare this experimental data with the FE model predictions and observe good agreement. Finally, we demonstrate iDEP particle trapping

using capillary-based fluid flow and compare trapping performance with that generated by the constant flow rate µPiP based DEP trapping. To the best of our knowledge, this is the first-time paper fibers have been used as insulating structures for dielectrophoretic trapping within paper pores. This new platform offers a budget-friendly method for iDEP-based applications for both academic prototyping and large-scale commercial device production.

2. Theory

In this work, we investigate the iDEP-based trapping of micron-scale particles within the pore spaces created by insulating glassy fibers in paper substates. We hypothesize that these insulating fibers can serve as sources of force-inducing dielectrophoresis field gradients for iDEP particle manipulations. When an electric field is applied across the paper channel, the paper fibers act as insulating structures and serve to induce electric field line curvature as the applied field is driven around each insulating fiber. Such localized curvature can be used to generate an electric field gradient for DEP. The DEP force acting on a spherical particle moving through the paper structure is dependent on this electric gradient and can be expressed as [36,37]:

$$\boldsymbol{F_{DEP} = 2\pi\varepsilon_o\varepsilon_m r^3 Re[K(\omega)]\nabla|E|^2}, \quad (1)$$

where, ε_o, ε_m, r and $\nabla|\mathrm{E}|^2$ are the permittivity of free space, dielectric constant of the media, the radius of the particle and the gradient of the electric field squared respectively and Re[K(ω)] is the real part of Clausius–Mossotti factor (CMF) [36,37]:

$$\mathbf{K(\omega)} = \frac{\varepsilon_p^* - \varepsilon_m^*}{\varepsilon_p^* + 2\varepsilon_m^*} \quad (2)$$

Here, in the absence of any net charge the electric field, *E*, is satisfied by the solution of the electric potential ($\boldsymbol{\phi}$) through the solution of the Laplace equation, $\boldsymbol{E = -\nabla\phi}$ Equation 2, describes the polarizability of a particle (p) in a medium (m) and is based on the complex permittivity ε*, which can be expressed as [37,38]:

$$\boldsymbol{\varepsilon^* = \varepsilon - i\frac{\sigma}{\omega}} \quad , \quad (3)$$

where, ε is the dielectric constant, and σ is the electrical conductivity of the medium and ω is the frequency. The complex K(ω) factor has an imaginary component which is out of phase with the applied electric field and exerts a torque on the particle that can be detected by particle electrorotation [38]. More importantly, the DEP force is dependent on the in phase real part of the K(ω) factor as shown in equation 1. In the case of DC dielectrophoresis, where frequency is zero, this factor can be expressed as [38]:

$$\lim_{\omega \to 0} \mathbf{K(\omega)} = \frac{\sigma_p - \sigma_m}{\sigma_p + 2\sigma_m} \quad (4)$$

In addition to the DEP force, a suspending particle flowing through a fluid at a given velocity, v experiences a drag force. For a pressure driven laminar fluid flow through a micron scale channel, the Navier-Stokes' equation can be simplified, and the drag force can be approximated by the following equation [39–41]:

$$\boldsymbol{F_{HD} = 6\pi\eta r v,} \quad (5)$$

where, η and v are the fluid viscosity and velocity respectively. The threshold and onset of trapping a moving particle by DEP occurs when the DEP force is equal to or greater than the drag force [40,41]. Therefore, a trapping zone inside the porous structure of paper is created when the following force balance criteria is satisfied:

$$\boldsymbol{F_{DEP} \geq F_{HD}} \quad (6)$$

In this work we investigate the ability to trap micro-scale polarizable particles using the insulating fibers within porous paper fluidic channels. To accomplish this, we perform both experimental and computational analysis of the iDEP trapping dynamics within a paper channel pore-space subjected to a steady flow of a particle suspension either through a pressure gradient or capillary wicking. In the next section we describe the fabrication process of these paper channel iDEP devices and the process in which we quantify their 3D structure using micro computed tomography (micro-CT) scans.

3. Methods

3.1 Device Fabrication

The fabrication workflow for paper based dielectrophoretic trapping device is based on our recently developed fabrication technique called microfluidic pressure in paper (μPiP) and is illustrated in figure 1 [24]. The entire fabrication process, from design to device takes less than 10 minutes to complete. The fabrication begins by first cutting a microfluidic straight channel geometry (4 mm wide, 40 mm long) from a sheet of Craneglas® 230 paper (Neenah Filtration) using a CO_2 laser cutter (LS-2440, Boss Laser). A set of two copper tape electrodes (9 mm wide, 30 mm long, 3M™) are placed on the axial direction of the paper channel with 1 mm gap between them. Each paper channel and copper tape electrodes are then sealed between two thin flexible polydimethylsiloxane (PDMS) sheets (0.5 mm, McMaster-Carr). Fluidic channel inlets/outlets are hole punched on the top PDMS sheet using a 0.75 mm biopsy punch (Ted Pella, Inc.). The two sheets are then oxidized and irreversibly bonded together using oxygen plasma generated with a handheld tesla coil (Electro-Technic Products, Model BD-20AC). Lastly, the sealed PDMS device is placed into a bench top heat press (Dulytek DW 400) at a temperature of 55°C for 5 minutes which remove all observable air gaps and bubbles surrounding the paper channel structure. Copper wires are used to connect electrodes to external a voltage generator. For the wicking experiment, a paper channel is placed on top of a PDMS sheet and adhesive copper tapes are placed in the axial direction as electrodes. The paper channels were soaked in 3% w/v BSA (Sigma) in diH_2O for twenty minutes and dried prior to experimental use.

3.2 Micro-CT Analysis of Paper Channels

Micro-CT scans of the paper substrate were captured in order to investigate the porous structure of the insulating fibers and the resulting distribution of both the electric field and DEP force. The SkyScan 1272 bench top micro-CT scan from Micro Photonics Inc. was used for paper CT scan imaging (1.5µm voxel size, 800 ms exposure time) and CTvox software was used to generate 3D images from the scanning results. The resulting micrograhs were digitally converted into a 3D structure and used as a computational domain for finite element analysis via a finite element Multiphysics software (COMSOL Inc., Burlington, MA).

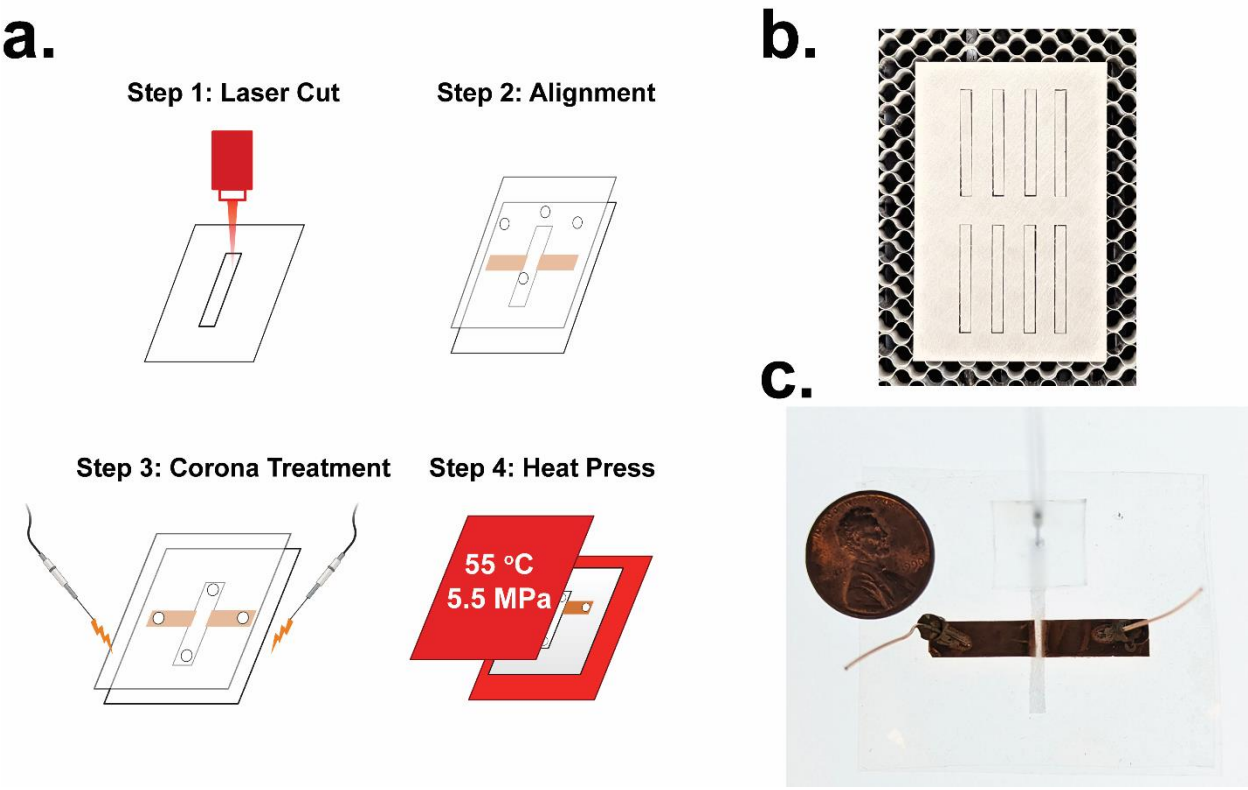

Figure 1: A) Fabrication workflow for paper based dielectrophoretic trapping device. B) Paper channels fabricated using CO_2 laser cut. C) Assembled device

3.3 Experimental Setup and Operation

DEP trapping experiments were performed using fluorescent polystyrene micro-particles (1µm diameter, Bangs Laboratories, Inc.). Polystyrene particles were suspended in deionized water and diluted to a concentration of 8×10^5 particles per mL, 5wt% Tween 20 was added to the solution to reduce particle agglomeration. A function generator (Rigol DG1022Z) was used to apply a pulsed DC electric field perpendicular to the flow direction. This positive-pulsed waveform served to significantly reduce the influence of Faradaic reactions and bubble nucleation in the paper channel, while providing the maximum average potential across the channel. In addition, a handheld thermal camera (FLIR TG165) was used to observe joule heating effect and no increase in temperature was observed at the operating voltage range (2-10 V). The waveform consisted of a pulsed

positive square wave, starting from a value of 0 volts and stepping up to a value of 10 volts at a frequency of 100 kHz and a duty cycle of 80%. For constant flow experiments, a syringe pump (Chemyx Fusion 100) was used to flow particle solution at a flow rate of 4 µL/min though the paper channel and for wicking experiment, 50µL of the solution was pipetted into the channel inlet zone.

4. Results and Discussion

4.1 Finite Element Analysis

In this section, we describe the finite element analysis method we developed to investigate particle trapping mechanism within the porous structure of paper. At first, a micro-CT scan image of the paper was taken using a benchtop CT scan and was converted into a 3D image as shown in figure 2b. As can be seen from the 3D image, the fiber orientation of the paper is anisotropic, i.e., the direction of fiber orientation is higher in one particular axis as compared to all other axes. To generate maximum gradient and minimum fluidic resistance, fluid flow was directed towards the fiber direction and electric field was applied across the direction of fiber orientation. Next, finite element analysis was used on this digitally captured domain in order to better understand the formation of electric field gradient zones within paper pores and the dynamics of the DEP force distribution as the electric field strength was applied increased. The model consist of a 2D representation of the paper porous structure generated from the 3D micro-CT image. This 2D approximation has been previously used to model electric field gradient in iDEP devices based on the approximation that electric potential is relatively consistent across the small depth of the fluidic channel [16,42]. The boundaries of the paper fiber structures were set as insulators and water was assigned into the bounded domain. On side of the paper structure, parallel to the fiber direction was defined as ground and a range of DC voltage potential (0-10 V) was applied on the other side. The distribution of electric potential was determined using Laplace equation [42]:

$$\boldsymbol{\nabla^2 \phi = 0} \quad (7)$$

Where, $\boldsymbol{\phi}$ is the electric potential and the electric field was determined by [42,43]:

$$\mathbf{E} = -\boldsymbol{\nabla \phi} \quad (8)$$

Figure 2c and d represents the results for the gradient of the electric field squared ($\nabla|\mathrm{E}|^2$) for both the paper structure and a traditional iDEP device. From the figures, it is evident that paper structures produce regions of high electric field gradient, similar to that of traditional iDEP devices that can be used to trap, isolate, and concentrate particles from a suspending medium.

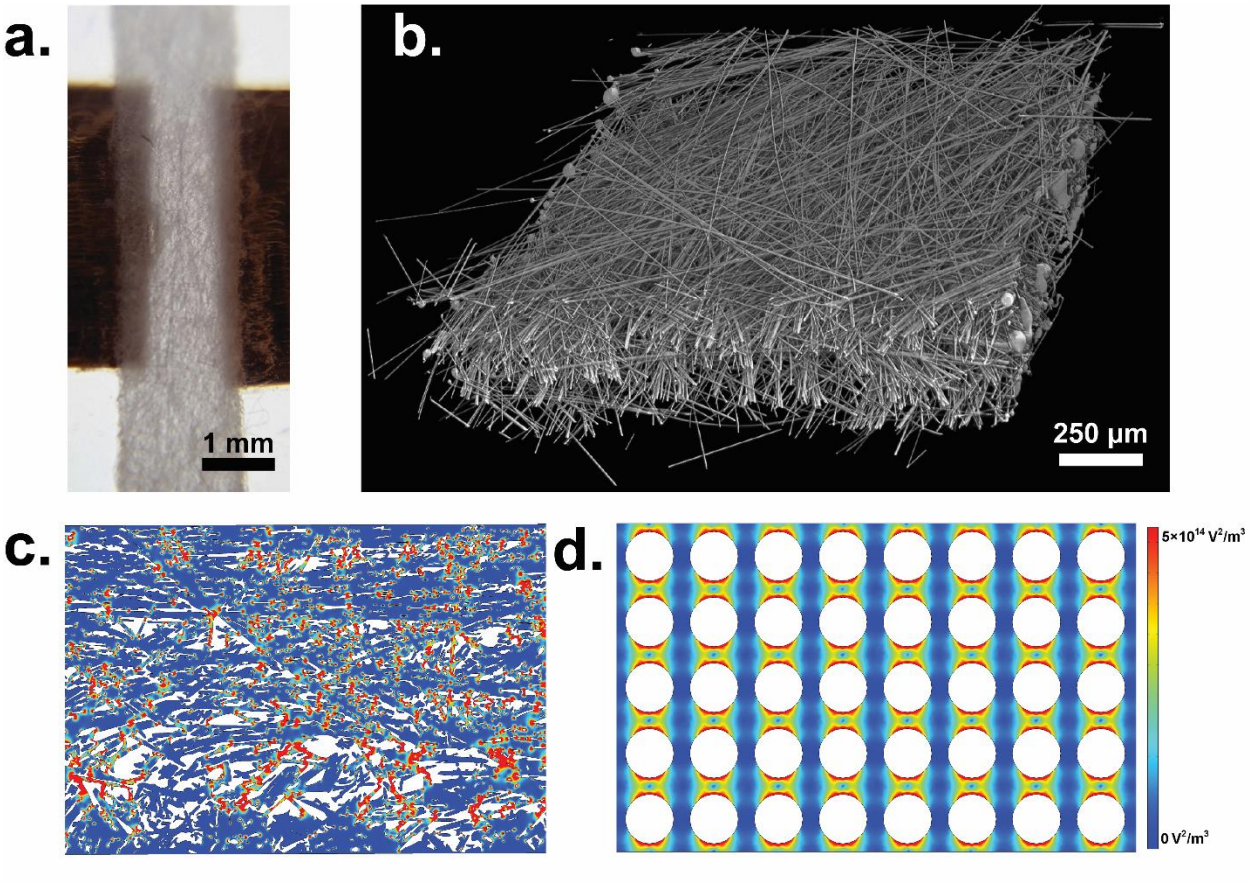

Figure 2: Proposed paper based iDEP device. A) The device used for particle trapping. B) Micro-CT scan of a paper based iDEP device. C) Electric field gradient distribution inside porous paper structure. D) Electric field gradient distribution in a traditional iDEP device

One key observation is that the electric field gradient produced in paper structure is more heterogenous (Fig. 2c) as compared to traditional insulating structures (Fig. 2d). The paper fibers consist of a wide variety of overlapping structures, ranging from parallel and perpendicularly aligned fibers that form porous flow regions and converging/diverging sharp and rounded fiber ends which occur at the entrance and exits to these flow regions. Previously it has been reported that, insulating structures with a sharp end, where the radius of curvature (ROC) changes rapidly, constrict the electric field and produce a larger electric field gradient as compared to rounded ends where ROC change is more gradual [4,42]. To better understand the DEP force growth dynamics in paper, increase in DEP force expressed as $\nabla|\mathrm{E}|^2$ with the increase in applied voltage at different trapping zones was measured using the COMSOL model as shown in figure 3a. Trapping zones are defined as specific locations within the paper structure with a high DEP force that are capable of trapping a moving particle. The color scheme was changed to blue and white to better illustrate trapping zone growth dynamics. From figure 3a, it can be seen that both the number of trapping zone and trapping domain, which is the volume where trapping occurs increase with the increase in applied voltage. While the DEP force in each trapping zone grows quadratically with applied voltage their growth rate is not the same.

DEP force in trapping zones with a sharp end grows faster than in zones with a more rounded end, as shown in figure 3b. To understand the bulk trapping dynamics, the average DEP force growth dynamics of 194 random trapping zones was measured (figure 3c) and plotted against applied voltage as shown in figure 3d. This average force growth curve shows a linear relationship with applied voltage (figure 3d).

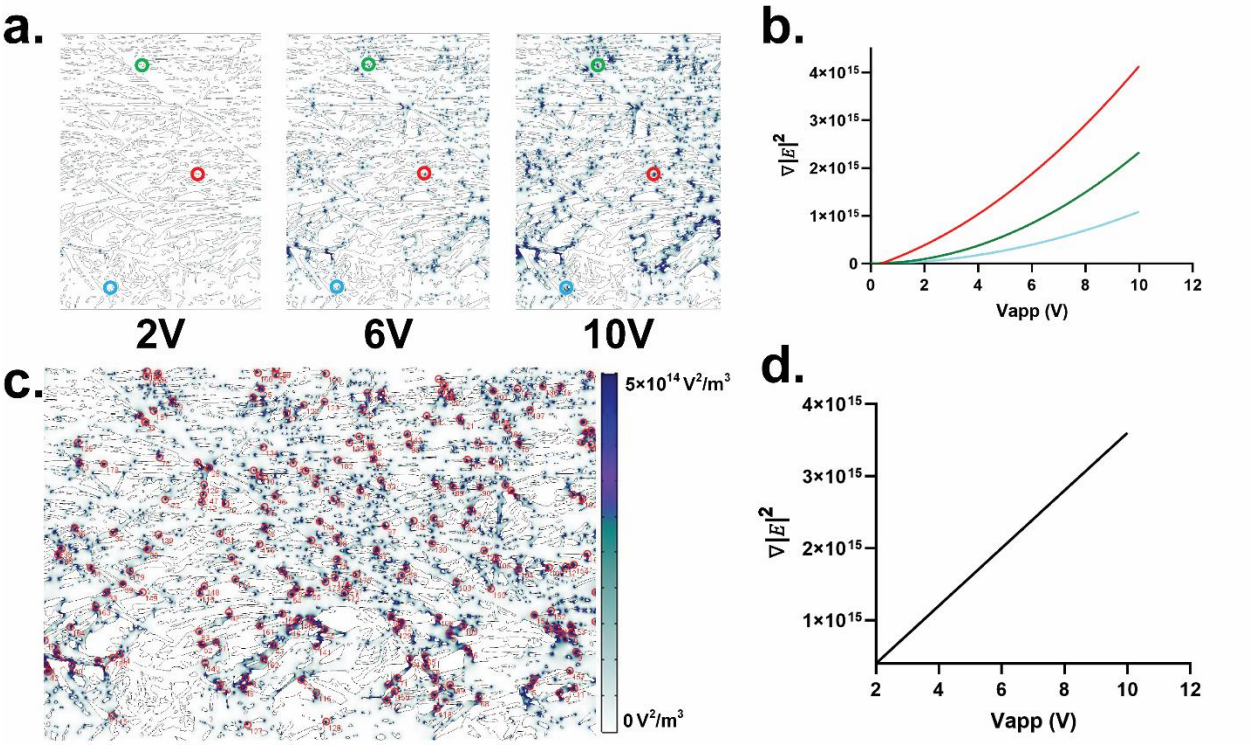

Figure 3: DEP force growth dynamics and trapping mechanism within paper pores. A) DEP force at different applied voltages within paper pores. B) DEP force growth curves for three different trapping zones. C) DEP trapping zones within paper pore D) Bulk force growth curve

4.2 Trapping Response to Voltage Change

We now present the experimental demonstration of the trapping behavior of paper structure using fluorescently labelled polystyrene (PS) particles. PS particles were flowed through paper at a constant flowrate of 4 µL/min and an external electric field was applied to trap the particles inside paper pores. The insulating paper structures generate zones of high electric field gradient that acts as barriers for the moving PS particles and trap them within paper pores. The number of particles trapped can be measured by monitoring the number and intensity of fluorescent spots generated for an applied electric field within the region of interest (red box, figure 4a). As shown in figure 4a, the number of particles trapped increases with the increases in applied field. To understand particle trap and release mechanism, the electric field was turned on for 70 seconds to trap particles and then turned off for 50 seconds to release the trapped particles. The resultant fluorescent intensity change with time was measured using imageJ software (ImageJ 1.47t). The applied voltage was increased from 2V up to 10V. As shown in figure 4b, as the field is turned on, the fluorescent intensity starts to increase and when the field is turned off the

intensity decreases. This demonstrates the trapping of PS particles occurs solely because of the applied field and when the field is turned off trapped particles are released. However, with time particle retention takes place within paper pores. In future studies, we will explore different surfactants and paper passivation mechanisms to understand paper particle interaction and develop procedures to reduce particle retention. In addition, the maximum amount of particle trapped for a given voltage was plotted and illustrated in figure 4c. The amount of particle trapped shows a linear relation with applied voltage as predicted by the finite element analysis described in section 4.1.

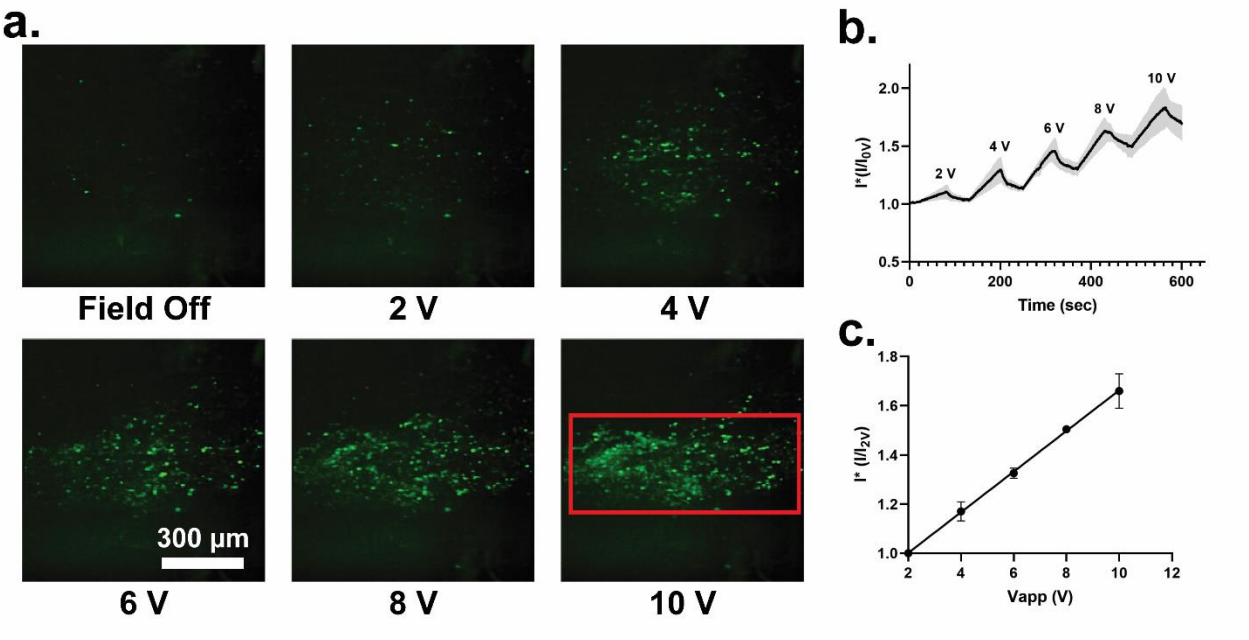

Figure 4: DEP particle trapping of fluorescently labeled PS particles. A) Particle trapping at different applied voltages. B) Particle capture and release data. C) Maximum fluorescent response at different applied voltages (one standard deviation error bar for n = 5 measurements).

4.3 Comparison Between Constant Flowrate and Capillary Flow

One major advantage that paper-based devices have is the ability to flow fluid by capillary action and thus enabling the development pump-free fluidic devices. In this section, we present dielectrophoretic particle trapping in paper by capillary action and compare the results with constant flowrate. 50 µL of PS solution was pipetted into the inlet zone of the device shown in figure 5a. The fluid saturated the inlet zone and started flowing through the paper channel. As the fluid front crossed the electrodes, a 10V pulsed DC electric field was applied and the resultant change in fluorescent intensity was measured. The same experiment was repeated with the field turned off. Fluorescent images of the two sets of experiments are shown in figure 5b, which illustrates particle trapping in paper pores when the electric field is turned on. Next, the trapping mechanism between constant flowrate and capillary flow was compared. Fluid was flowed through open paper channel by capillary action and through a µPiP channel at a constant flowrate of 4µL/min. The resultant fluorescent intensity change was measured for 80 seconds for both sets of experiments. As shown in figure 5c, for constant flowrate the trapped particle intensity

increases linearly with time. This is because, for constant flowrate, there is a constant flux of particles entering the trapping zone and therefore, with time more and more particles get trapped. For capillary flow, excluding surface evaporation, the flowrate can be approximated using Lucas-Washburn equation where the fluid flow is proportional to the square root of time ($t^{1/2}$) [24]. Therefore, with time, the flux of particles entering the trapping zone decreases and nears a plateau which is conveyed by the fluorescent intensity data. In addition, intensity data for capillary flow when the field is turned off is included in figure 4c, that shows no increase in fluorescent intensity. This demonstrates that particles are trapped solely by dielectrophoretic force and gravitational and mechanical trapping do not play any role for our system.

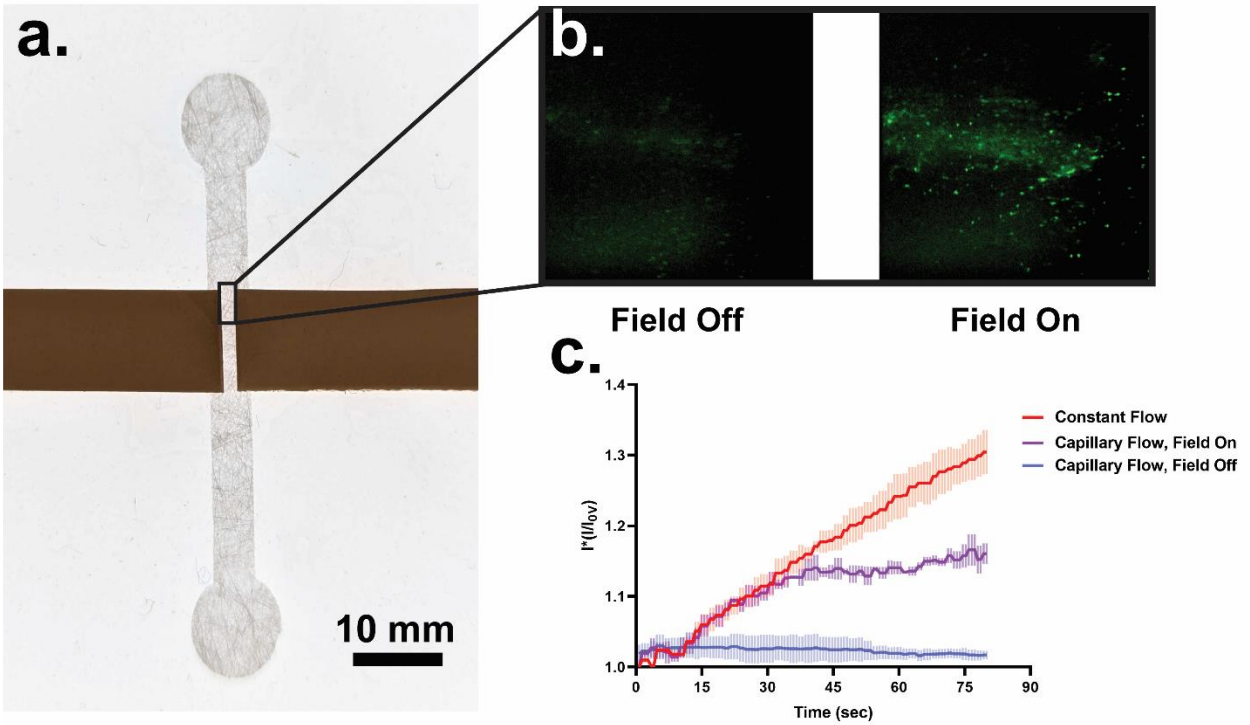

Figure 5: DEP particle trapping using passive fluid flow by capillary action. A) Proposed capillary action-based device. B) Particle trapping at 10V. C) Comparison Dep particle trapping between constant pressure-based fluid flow with capillary driven flow (one standard deviation error bar for n = 3 measurements).

5. Conclusion

In conclusion, we have demonstrated a novel paper-based DEP mechanism that uses the insulating nature of paper fibers to generate zones of high DEP force within paper structure. These trapping zones can be used to trap and concentrate particles. We have developed a finite element analysis method that can accurately predict DEP force growth dynamics and trapping mechanism within paper pores. We have also demonstrated particle trapping using two different fluid flow mechanisms, one with a constant flow rate and another with capillary action and compared trapping rate between the two mechanisms. Paper is low-cost, biocompatible, user friendly and biodegradable. Future work will demonstrate the biocompatibility paper-based DEP devices that can be used to

separate and concentrate the analyte of interest from a biofluid. We believe this novel paper-DEP method has immediate applications in a wide variety of areas such as disease diagnostics, microbial contamination detection, and public health monitoring. With further development, this technique will democratize DEP-based innovations by significantly reducing fabrication costs and enable manufacturing of robust devices at commercial scale.

Acknowledgements

The PI gratefully acknowledges support from a NASA Early Career Faculty award (80NSSC19K1401) and NSF I Corps award (2112224).

Reference

[1] S. Masuda, M. Washizu, T. Nanba, Novel Method Of Cell Fusion In Field Constriction Area In Fluid Integrated Circuit, IEEE Transactions on Industry Applications. 25 (1989) 732–737. https://doi.org/10.1109/28.31255.

[2] E.B. Cummings, A.K. Singh, Dielectrophoretic trapping without embedded electrodes, Microfluidic Devices and Systems III. 4177 (2000) 151–160. https://doi.org/10.1117/12.395653.

[3] C.F. Chou, J.O. Tegenfeldt, O. Bakajin, S.S. Chan, E.C. Cox, N. Darnton, T. Duke, R.H. Austin, Electrodeless dielectrophoresis of single- and double-stranded DNA, Biophysical Journal. 83 (2002) 2170–2179. https://doi.org/10.1016/S0006-3495(02)73977-5.

[4] A. LaLonde, A. Gencoglu, M.F. Romero-Creel, K.S. Koppula, B.H. Lapizco-Encinas, Effect of insulating posts geometry on particle manipulation in insulator based dielectrophoretic devices, Journal of Chromatography A. 1344 (2014) 99–108. https://doi.org/10.1016/j.chroma.2014.03.083.

[5] J.I. Martínez-López, H. Moncada-Hernández, J.L. Baylon-Cardiel, S.O. Martínez-Chapa, M. Rito-Palomares, B.H. Lapizco-Encinas, J.I. Martínez-López, J.L. Baylon-Cardiel, S.O. Martínez-Chapa, Characterization of electrokinetic mobility of microparticles in order to improve dielectrophoretic concentration, Anal Bioanal Chem. 394 (2009) 293–302. https://doi.org/10.1007/s00216-009-2626-y.

[6] H. Moncada-Hernández, B.H. Lapizco-Encinas, Simultaneous concentration and separation of microorganisms: Insulator-based dielectrophoretic approach, Analytical and Bioanalytical Chemistry. 396 (2010) 1805–1816. https://doi.org/10.1007/s00216-009-3422-4.

[7] N. Hill, A.C. de Peña, A. Miller, B.H. Lapizco-Encinas, On the potential of microscale electrokinetic cascade devices, Electrophoresis. 42 (2021) 2474–2482. https://doi.org/10.1002/elps.202100069.

[8] S.K. Srivastava, A. Artemiou, A.R. Minerick, Direct current insulator-based dielectrophoretic characterization of erythrocytes: ABO-Rh human blood typing, Electrophoresis. (2011) 2530–2540. https://doi.org/10.1002/elps.201100089.

[9] A. Salmanzadeh, M.B. Sano, R.C. Gallo-Villanueva, P.C. Roberts, E.M. Schmelz, R. v. Davalos, Investigating dielectric properties of different stages of syngeneic murine ovarian cancer cells, Biomicrofluidics. 7 (2013). https://doi.org/10.1063/1.4788921.

[10] M.B. Sano, J.L. Caldwell, R. v. Davalos, Modeling and development of a low frequency contactless dielectrophoresis (cDEP) platform to sort cancer cells from dilute whole blood samples, Biosensors and Bioelectronics. 30 (2011) 13–20. https://doi.org/10.1016/j.bios.2011.07.048.
[11] H. Shafiee, M.B. Sano, E.A. Henslee, J.L. Caldwell, R. v. Davalos, Selective isolation of live/dead cells using contactless dielectrophoresis (cDEP), Lab on a Chip. 10 (2010) 438–445. https://doi.org/10.1039/b920590j.
[12] A. Salmanzadeh, L. Romero, H. Shafiee, R.C. Gallo-Villanueva, M.A. Stremler, S.D. Cramer, R. v. Davalos, Isolation of prostate tumor initiating cells (TICs) through their dielectrophoretic signature, Lab on a Chip. 12 (2012) 182–189. https://doi.org/10.1039/c1lc20701f.
[13] M.D. Pysher, M.A. Hayes, Electrophoretic and dielectrophoretic field gradient technique for separating bioparticles, Analytical Chemistry. 79 (2007) 4552–4557. https://doi.org/10.1021/ac070534j.
[14] J. Ding, C. Woolley, M.A. Hayes, Biofluid pretreatment using gradient insulator-based dielectrophoresis: separating cells from biomarkers, Analytical and Bioanalytical Chemistry. 409 (2017) 6405–6414. https://doi.org/10.1007/s00216-017-0582-5.
[15] P. v Jones, S. Huey, P. Davis, R. Mclemore, A. Mclaren, M.A. Hayes, Biophysical separation of Staphylococcus epidermidis strains based on antibiotic resistance, Analyst. 140 (2015) 5152. https://doi.org/10.1039/c5an00906e.
[16] J. Ding, R.M. Lawrence, P. v. Jones, B.G. Hogue, M.A. Hayes, Concentration of Sindbis virus with optimized gradient insulator-based dielectrophoresis, Analyst. 141 (2016) 1997–2008. https://doi.org/10.1039/c5an02430g.
[17] S.J.R. Staton, P. v Jones, G. Ku, S.D. Gilman, I. Kheterpal, M.A. Hayes, Manipulation and capture of Ab amyloid fibrils and monomers by DC insulator gradient dielectrophoresis (DC-iGDEP) †, (n.d.). https://doi.org/10.1039/c2an35138b.
[18] B.G. Abdallah, T.-C. Chao, C. Kupitz, P. Fromme, A. Ros, Dielectrophoretic Sorting of Membrane Protein Nanocrystals, (2013). https://doi.org/10.1021/nn403760q.
[19] B.G. Abdallah, S. Roy-Chowdhury, J. Coe, P. Fromme, A. Ros, High Throughput Protein Nanocrystal Fractionation in a Microfluidic Sorter, (2015). https://doi.org/10.1021/acs.analchem.5b00589.
[20] P. v Jones, G.L. Salmon, A. Ros, Continuous Separation of DNA Molecules by Size Using Insulator-Based Dielectrophoresis, Anal. Chem. 89 (2017) 21. https://doi.org/10.1021/acs.analchem.6b03369.
[21] G.R. Pesch, M. Lorenz, S. Sachdev, S. Salameh, F. Du, M. Baune, P.E. Boukany, J. Thöming, Bridging the scales in high-throughput dielectrophoretic (bio-) particle separation in porous media OPEN, (n.d.). https://doi.org/10.1038/s41598-018-28735-w.
[22] G.R. Pesch, F. Du, U. Schwientek, C. Gehrmeyer, A. Maurer, J. Thöming, M. Baune, Recovery of submicron particles using high-throughput dielectrophoretically switchable filtration, Separation and Purification Technology. 132 (2014) 728–735. https://doi.org/10.1016/j.seppur.2014.06.028.

[23] M. Lorenz, D. Malangré, F. Du, M. Baune, J. Thöming, G.R. Pesch, High-throughput dielectrophoretic filtration of sub-micron and micro particles in macroscopic porous materials, Analytical and Bioanalytical Chemistry. 412 (2020) 3903–3914. https://doi.org/10.1007/s00216-020-02557-0.
[24] M.N. Islam, J.W. Yost, Z.R. Gagnon, Microfluidic pressure in paper (μPiP): Rapid prototyping and low-cost liquid handling for on-chip diagnostics, Analyst. 147 (2022). https://doi.org/10.1039/d1an01676h.
[25] M.N. Islam, I. Ahmed, M.I. Anik, M.S. Ferdous, M.S. Khan, Developing Paper Based Diagnostic Technique to Detect Uric Acid in Urine, Front Chem. 6 (2018) 496. https://doi.org/10.3389/fchem.2018.00496.
[26] A.W. Martinez, S.T. Philips, G.M. Whitesides, E. Carrilho, Diagnostics for the Developing World: Microfluidic Paper-Based Analytical Devices, Analytical Chemistry. (2010) 3–10.
[27] C.M. Cheng, A.W. Martinez, J. Gong, C.R. Mace, S.T. Phillips, E. Carrilho, K.A. Mirica, G.M. Whitesides, Paper-based ELISA, Angew Chem Int Ed Engl. 49 (2010) 4771–4774. https://doi.org/10.1002/anie.201001005.
[28] P. Mandal, R. Dey, S. Chakraborty, Electrokinetics with “paper-and-pencil” devices., Lab Chip. 12 (2012) 4026–4028. https://doi.org/10.1039/c2lc40681k.
[29] Y. Matsuda, K. Sakai, H. Yamaguchi, T. Niimi, Electrophoretic separation on an origami paper-based analytical device using a portable power bank, Sensors (Switzerland). 19 (2019). https://doi.org/10.3390/s19071724.
[30] Y.Q. Liu, B. Ji, X.H. Yan, S. Lv, F. Fang, X.L. Guo, Z.Y. Wu, Fast and highly efficient multiplexed electrokinetic stacking on a paper-based analytical device, Microchemical Journal. 174 (2022) 107041. https://doi.org/10.1016/j.microc.2021.107041.
[31] B.Y. Moghadam, K.T. Connelly, J.D. Posner, Isotachophoretic Preconcenetration on Paper-Based Microfluidic Devices, Anal. Chem. 86 (2014). https://doi.org/10.1021/ac500780w.
[32] R. Dey, S. Kar, S. Joshi, T.K. Maiti, S. Chakraborty, Ultra-low-cost ‘paper-and-pencil’ device for electrically controlled micromixing of analytes, Microfluidics and Nanofluidics. 19 (2015) 375–383. https://doi.org/10.1007/s10404-015-1567-3.
[33] S.S. Das, S. Kar, S. Dawn, P. Saha, S. Chakraborty, Electrokinetic Trapping of Microparticles Using Paper-and-Pencil Microfluidics, Physical Review Applied. 12 (2019) 1. https://doi.org/10.1103/PhysRevApplied.12.054017.
[34] I. Electrolock, CraneGlass 230 Data Sheet, 2009.
[35] Neenah Filtration, Glass wet-laid nonwovens - Craneglas®, (n.d.). https://www.neenah-filtration.com/materials-technologies/glass-nonwovens/ (accessed July 4, 2022).
[36] R. Pethig, Dielectrophoresis: Status of the theory, technology, and applications, Biomicrofluidics. 4 (2010) 1–35. https://doi.org/10.1063/1.3456626.
[37] E. Lavi, F. Crivellari, Z. Gagnon, Dielectrophoretic detection of electrical property changes of stored human red blood cells _ Enhanced Reader, Electrophoresis. (2022).
[38] A.R. Minerick, DC Dielectrophoresis in Lab-on-a-Chip Devices., In: Li D. (Eds) Encyclopedia of Microfluidics and Nanofluidics. Springer, Boston, MA. (2008). https://doi.org/10.1007/978-0-387-48998-8_294.

[39] N. Piacentini, G. Mernier, R. Tornay, P. Renaud, Separation of platelets from other blood cells in continuous-flow by dielectrophoresis field-flow-fractionation, Biomicrofluidics. 5 (2011). https://doi.org/10.1063/1.3640045.
[40] M. Li, S. Li, W. Cao, W. Li, W. Wen, G. Alici, Improved concentration and separation of particles in a 3D dielectrophoretic chip integrating focusing, aligning and trapping, (n.d.). https://doi.org/10.1007/s10404-012-1071-y.
[41] J. Cao, P. Cheng, F. Hong, A numerical analysis of forces imposed on particles in conventional dielectrophoresis in microchannels with interdigitated electrodes, Journal of Electrostatics. 66 (2008) 620–626. https://doi.org/10.1016/j.elstat.2008.09.003.
[42] C. v. Crowther, M.A. Hayes, Refinement of insulator-based dielectrophoresis, Analyst. 142 (2017) 1608–1618. https://doi.org/10.1039/c6an02509a.
[43] D. Chen, H. Du, A microfluidic device for rapid concentration of particles in continuous flow by DC dielectrophoresis, (n.d.). https://doi.org/10.1007/s10404-009-0545-z.